Third Harmonic Generation Enhanced by Multipolar Interference in Complementary Silicon Metasurfaces

Chen, Shumei; Rahmani, Mohsen; Li, King Fai; Miroshnichenko, Andrey; Zentgraf, Thomas; Li, Guixin; Neshev, Dragomir; Zhang, Shuang

DOI:
10.1021/acsphotonics.7b01423

Document Version
Peer reviewed version

Citation for published version (Harvard):
Chen, S, Rahmani, M, Li, KF, Miroshnichenko, A, Zentgraf, T, Li, G, Neshev, D & Zhang, S 2018, 'Third Harmonic Generation Enhanced by Multipolar Interference in Complementary Silicon Metasurfaces', ACS Photonics. https://doi.org/10.1021/acsphotonics.7b01423

Third harmonic generation enhanced by multipolar interference in complementary silicon metasurfaces

Shumei Chen[1♀], Mohsen Rahmani[2♀], King Fai Li[3], Andrey Miroshnichenko[4], Thomas Zentgraf[5], Guixin Li[3,6*], Dragomir Neshev[2*], Shuang Zhang[1*]

[1]School of Physics and Astronomy, University of Birmingham, Birmingham, B15 2TT, UK

[2]Nonlinear Physics Centre, Research School of Physics and Engineering, The Australian National University, Canberra, ACT 2601, Australia

[3]Department of Materials Science and Engineering, Southern University of Science and Technology, Shenzhen, 518055, China

[4]School of Engineering and Information Technology, University of New South Wales - Canberra, Northcott Drive, Campbell, ACT 2600, Australia

[5]Department of Physics, University of Paderborn, Warburger Strasse 100, D-33098 Paderborn, Germany

[6]Institute for Quantum Science and Engineering, Southern University of Science and Technology, Shenzhen, 518055, China

* Corresponding author: ligx@sustc.edu.cn; Dragomir.Neshev@anu.edu.au; s.zhang@bham.ac.uk

Abstract

Nonlinear harmonic generation in metasurfaces has shown great promises for applications such as novel light sources, nonlinear holography and nonlinear imaging. In particular, dielectric metasurfaces have shown multi-fold enhancement of the harmonic efficiency in comparison to their plasmonic counterparts due to lower optical loss and much higher damage threshold. In this work, we propose to enhance the efficiency of the third harmonic generation in a complementary silicon nonlinear metasurface, consisting of nanoapertures of cross-like shape in the silicon film. The efficiency enhancement is based on a multipolar interference between the magnetic dipole and electric quadrupole, resulting in significant near-field enhancement and a large mode volume of the nonlinear interaction. The measured efficiency of third harmonic generation from the silicon metasurface is 100 times higher than that from a planar silicon film of the same thickness. Numerical analysis of the near-field resonant modes confirms the multipolar mechanism of nonlinear enhancement. Enhanced third harmonic generation by multipolar interference in complementary dielectric nanostructure opens a new route for developing high-efficiency nonlinear metasurfaces.

Key Words

Metasurfaces, Nonlinear Optics, Silicon Photonics, Waveguide, Third Harmonic Generation

Silicon photonic circuits, which are compatible with mature CMOS technologies, show great potential for on-chip information processing and thus have attracted attention from both academic and industry communities.[1] To modulate the optical signals in silicon devices, various nonlinear optical (NLO) processes have been used, such as the frequency conversion processes stemming from the third order susceptibility of silicon, light amplification based on Raman scattering and four-wave mixing, as well as in all-optical de-multiplexing etc.[2,3] However, one of the key obstacles that limits the applications of nonlinear silicon device is its low NLO efficiency. To circumvent this constraint, strong light localization in photonic crystal or plasmonic device has been proposed as viable path to greatly enhance the NLO efficiency.[4-6] For example, plasmonic nanostructures with strong light-matter interaction in the sub-wavelength volume have been utilized to enhance the efficiency of second harmonic generation (SHG),[7-14] third harmonic generation (THG),[15-20] and four-wave mixing.[21-23] Unfortunately, both metal and metal-silicon hybrid plasmonic devices inherit some intrinsic disadvantages of noble metals, i.e. high loss and low damage threshold. In comparison, silicon nanostructures are exempt from these problems. Two-dimensional silicon photonic crystals have been designed to exhibit strong THG based on slow light and cavity effect.[24,25]

More recently, silicon nanoparticles were suggested as a promising platform for enhancing the NLO processes due to strong confinement of light at the magnetic dipole resonance.[26-31] It was shown that silicon nanoparticles of a few hundred nanometers thick can result in a very large THG efficiency of the order of ~10^{-7}, which is ultimately limited by the two-photon absorption and the damage threshold of silicon. Further ideas for harmonic efficiency enhancement have been explored, including Fano resonances,[27,29] anapole modes,[32,33] hybrid antennas[34] and Germanium antennas as higher nonlinear material, leading to efficiencies

of up to 10^{-5}. These techniques however suffer from the small mode volume of the nanoantenna. Here we propose a new scheme for achieving strong third harmonic nonlinear conversion in a metasurface featuring an extended mode volume that greatly facilitates the nonlinear interaction of light.

Results and Discussions

Here, we adopt a complementary silicon metasurface, which consists of a 2D periodic array of nanoapertures, as schematically shown in Fig. 1. Such nanostructure was introduced in the concept of all-dielectric metasurfaces in Ref.35 and was shown to exhibit a rich variety of modes, including leaky guided mode, dark and bright multipolar modes. When the fundamental wave (FW) is normally incident onto the metasurface, the hole-array can couple the incident wave into different multipolar modes. The interference between the guided and localized modes in the structure results in Fano-type spectral resonant features, where the near field are strongly enhanced, allowing to dramatically increase the THG by the metasurface. The proposed silicon metasurface represents a facile approach towards highly efficient THG sources.

Here we fabricate the silicon metasurface on a fused silica substrate, which suffers much less of TPA effect than a silicon substrate. Fig. 1(b) shows the scanning electron microscopy image of the silicon metasurface consisting of a periodic array of silicon nanoapertures. The silicon metasurface is fabricated using electron beam lithography. A 205 nm thick amorphous silicon film is deposited on a 200 μm thick fused silica substrate via a plasma enhanced chemical vapor deposition (PECVD) process. Next, an electron beam resist with a thickness of 200 nm is spin-coated onto the silicon film, followed by electron beam patterning of periodic nanoapertures. Finally, the silicon film is etched under the protection of resist mask and silicon nanoapertures with periodicities of 600 nm in both x- and y-axis directions are obtained.

Numerical calculations are performed using Lumerical finite difference time-domain (FDTD) software. Our simulations allow us to obtain both the multipolar decomposition and near-field distributions. The calculated transmittance spectrum is shown in Fig. 1(c) with red line and closed squires. The simulations match the resonance behaviour reasonably well, where the resonant mode appears at a wavelength around 1296 nm. We then characterize the linear optical properties of the silicon planar thin film and metasurface by using Fourier transformation infrared spectrometry. As shown in Fig. 2(b), in the measured transmittance spectrum (open red circles) we observe a clear transmission dip at a wavelength of 1281 nm, which is a result of excitation of resonant modes in the complementary silicon structure. The measured resonant dip is broader than the simulated one, which can be attributed to the imperfection of nanofabrication and the large numerical aperture (N.A. = 0.36) objective lens used for the transmission measurement.

Fig. 2(a) shows the calculated multipolar decomposition for our structure. We calculate the Cartesian multipoles up to the third order based on the electric field **E** inside the unit cell. Based on the multipolar expansion of the polarization current density, the multipole terms (electric dipole **p**, magnetic dipole **m** and electric quadrupole $\mathbf{Q_e}$) are calculated according to the following equations:

$$\mathbf{p} = \varepsilon_0 (1-\varepsilon) \int \mathbf{E} d^3 r,$$

$$\mathbf{m} = \frac{i\omega}{2} \varepsilon_0 (1-\varepsilon) \int \mathbf{r} \times \mathbf{E} d^3 r,$$

$$Q_{\alpha\beta} = \frac{\varepsilon_0 (1-\varepsilon)}{2} \int \left[r_\alpha E_\beta + r_\beta E_\alpha - \frac{2}{3} \delta_{\alpha\beta} (\mathbf{r} \cdot \mathbf{E}) \right] d^3 r.$$

where ω is the angular frequency, ε_0 is the vacuum permittivity and ε are the relative permittivity of the silicon. The total scattered power P_{total} is calculated as the sum of each multipole contributions:

$$P_{\text{total}} \; ; \; \frac{c^2 k_0^4 Z_0}{12\pi}|\mathbf{p}|^2 + \frac{k_0^4 Z_0}{12\pi}|\mathbf{m}|^2 + \frac{c^2 k_0^6 Z_0}{40\pi}\sum|Q_{\alpha\beta}|^2,$$

with k_0 being the wave number, and Z_0 being the wave impedance in the vacuum. [36]

It is found that the electric quadrupole and magnetic dipole are the two dominant modes contributing to the resonant behaviour. The dominant magnetic dipole mode is in the plane of the metasurface and can couple to both in-plane (inside the silicon slab) and to free-space (radiating) modes. The quadrupolar mode does not couple to free-space radiation directly but only through coupling with the magnetic dipole mode. The spectral position of maximal scattering between the magnetic dipole and quadrupole modes is slightly displaced due to the interaction of both modes with the weaker in-plane electric dipole mode (black curve in Fig. 2(a)). Interestingly, both the magnetic dipole and the electric quadrupole components exhibit an asymmetric line-shape, which is a result of the interference between the radiative and guided modes in the silicon slab. To illustrate the mode structure, in Figs. 2(b) and (c) we show the components of electric field E_x and magnetic field H_y in a unit cell of the silicon metasurface at the FW of 1287 nm in the X-Y plane (z=0), which corresponds to the peak efficiency THG in Fig. 4. From the field distribution in Fig. 2(c), the electric quadrupole and magnetic dipole patterns at fundamental wave of 1287 nm are clearly observed from the four petals and two petals in the distributions of electric field and magnetic field, respectively. As expected, the fundamental wave is strongly localized inside silicon when the guided mode is excited.

To better understand the waveguide mode enhanced THG from the silicon metasurface and planar thin film, nonlinear optical calculation is performed based on the linear response of the metasurface at both the fundamental and third harmonic wavelengths.[20] In the calculation, the third-order susceptibility $\chi^{(3)}$ of amorphous silicon is assumed to be dispersionless for the FW between 1.2 μm and 1.34 μm and the third order susceptibility of air is neglect. The far-field

THG intensity is calculated by the following steps: first, the electric field distribution in a unit cell of the silicon metasurface is simulated at both fundamental and THG wavelengths by using TM (H-)- polarized plane waves. Next, since the silicon is homogenous at each local point r, the $\chi^{(3)}$ tensor becomes a simple constant and thus the nonlinear polarization is written as $P_{THG}(r) = \chi^{(3)} \cdot \vec{E}(r) \cdot \vec{E}(r) \cdot \vec{E}(r)$. Finally, the induced nonlinear polarization emits radiation to the far-field, which can be described by using the Green's function $\overleftrightarrow{G}(r', r)$ at the THG wavelength and the total intensity is given by:

$$I = \left| \vec{E}_{total}(r') \right|^2 = \left| \int \overleftrightarrow{G}(r', r) \cdot \vec{P}_{THG}(r) d^3 r \right|^2 \qquad \text{Eq.1}$$

As shown in Fig. 3(a)-(c), the amplitude and phase distributions of FW and THG wave, and the term $\overleftrightarrow{G}(r', r) \cdot \vec{P}_{THG}(r)$ at each local point are averaged for different Z position and plotted in the X-Y plane for FW at wavelengths of 1287 nm, which corresponds to the peak THG efficiency in the calculated nonlinear response (Fig. 4d). It is clearly observed that the amplitude of the nonlinear polarizations that contribute to the far field is strongly localized inside the silicon metasurface.

The THG from the silicon planar film and metasurface is measured using a spectrally tunable femtosecond laser source (repetition frequency: 82 MHz, pulse duration: ~ 200 fs). The fundamental wave with a spot size of ~ 20 μm in diameter was normally incident onto the silicon metasurface after passing through an objective lens (N.A. = 0.1). The THG signals in transmission direction are collected by an infinity-corrected objective lens (N.A.=0.5) onto an Andor spectrometer (SP500i) with a photomultiplier tube detector. For a linearly (TM: H) polarized FW at a wavelength of 1280 nm (Fig. 4(a)), the intensity of THG signal with the TM polarization (H) is much stronger than that with TE polarization (V). For the H-H measurement

(Fig. 4(b)), the intensity of THG at the wavelength of 432 nm shows a cubic dependence upon the pumping power of the FW, suggesting that the signal indeed results from a third-order nonlinear optical process. Fig. 4(c) shows the far field radiation pattern of waveguide mode enhanced THG, which was captured by a colour CCD camera in the *k*-space.

Subsequently, we study the spectral dependence of THG efficiency, defined by $\eta = I_{THG}/I_{FW}$, from both the silicon planar film and metasurface by tuning the wavelength of FW from 1.2 μm to 1.34 μm. At the fundamental wavelength of 1280 nm, the measured THG efficiency from the silicon metasurface (solid squares) has an enhancement factor up to 220 with respect to that from the planar silicon film (solid triangles). This observed enhancement of the THG signal arises from the strong field enhancement inside the silicon metasurface. This is confirmed by the observation that the peak THG efficiency occurs at waveguide resonant wavelength of 1280 nm. For the H-polarized FW with an averaged pumping power of 26.7 mW, the maximum efficiency of the THG with a value of 1.76×10^{-7} is also obtained. This nonlinear optical conversion efficiency is comparable to the value measured from silicon nanoresonators at comparable pumping density.[26,27] As shown in Fig. 4(d), the calculated efficiency of spectrally resolved THG (open squares and triangles) agree reasonably well with the measurement results. It is found that the calculated THG efficiency reaches the maximum for fundamental wavelength at 1287 nm. The THG intensity from the silicon metasurface has an enhancement factor up to ~ 953 with respect to that from the planar silicon film. The discrepancy between the measurement and simulation is mainly due to the imperfections in the nanofabrication of the metasurface. For the fundamental wave with wavelength around 1200 nm-1230 nm, the measured THG efficiency is higher than the calculated value. This may be attributed to the presence of unintended modes introduced by the imperfection in the nano-fabrication of the silicon metasurface.

Conclusions

We have shown that the guided mode in silicon metasurface can be utilized to greatly enhance the THG efficiency. The THG experiment was performed on a silicon photonic device with an area size of 900 μm^2 and thickness of ~ 200 nm. Thus, the proposed silicon metasurface provides a compact platform for manipulating the nonlinear optical processes. We also implemented the nonlinear optical calculation procedures which exactly predict the measured THG efficiency from both a silicon planar thin film and the metasurface. We note that the measured THG efficiency is obtained using resonant modes of moderate quality factors and might not be the highest possible for our complementary structure. We believe that the efficiency could be further improved by designing sharper Fano resonances in the silicon metasurface. More importantly, the concept of THG enhancement in this work can be used to design various nonlinear functional silicon photonic circuits.

References

(1) Priolo, F.; Gregorkiewicz, T.; Galli, M.; Krauss, T. F. Silicon nanostructures for photonics and photovoltaics. *Nat. Photon*. **2014**, *9*, 19-32.

(2) Leuthold, J.; Koos, C.; Freude, W. Nonlinear silicon photonics. *Nat. Photon.* **2010**, *4*, 535-544.

(3) Boyd, R. W. *Nonlinear Optics*; Academic Press; San Diego, USA 2008.

(4) Kauranen, M.; Zayats, A. V. Nonlinear plasmonics. *Nat. Photon.* **2012**, *6*, 737-748.

(5) Lapine, M.; Shadrivov, I. V.; Kivshar, Y. S. Colloquium: Nonlinear metamaterials. *Rev. Mod. Phys.* **2014**, *86*, 1093-1123.

(6) Li, G.; Zhang, S.; Zentgraf, T. Nonlinear Photonic Metasurfaces. *Nat. Rev. Mater.* **2017**, *3*, 17010.

(7) Kujala, S.; Canfield, B. K.; Kauranen, M.; Svirko, Y.; Turunen, J. Multipole interference in the second-harmonic optical radiation from gold nanoparticles. *Phys. Rev. Lett.* **2007**, *98*, 167403.

(8) Valev, V. K.; Silhanek, A. V.; Verellen, N.; Gillijns, W.; Van Dorpe, P.; Aktsipetrov, O. A.; Vandenbosch, G. A. E.; Moshchalkov, V. V.; Verbiest, T. Asymmetric Optical Second-Harmonic Generation from Chiral G-Shaped Gold Nanostructures. *Phys. Rev. Lett*. **2010**, *104*, 127401.

(9) Zhang, Y.; Grady, N. K.; Ayala-Orozco, C.; Halas, N. J. Three-dimensional nanostructures as highly efficient generators of second harmonic light. *Nano Lett.* **2011**, *11*, 5519-5523.

(10) Cai, W.; Vasudev, A. P.; Brongersma, M. L. Electrically controlled nonlinear generation of light with plasmonics. *Science* **2011**, *333*, 1720-1723.

(11) Czaplicki, R.; Husu, H.; Siikanen, R.; Makitalo, J.; Kauranen, M. Enhancement of second-harmonic generation from metal nanoparticles by passive elements. *Phys. Rev. Lett.* **2013**, *110*, 093902.

(12) Konishi, K.; Higuchi, T.; Li, J.; Larsson, J.; Ishii, S.; Kuwata-Gonokami, M. Polarization-Controlled Circular Second-Harmonic Generation from Metal Hole Arrays with Threefold Rotational Symmetry. *Phys. Rev. Lett.* **2014**, *112*, 135502.

(13) O'Brien, K.; Suchowski, H.; Rho, J.; Salandriona, A.; Kante, B.; Yin, X.; Zhang, X. Predicting nonlinear properties of metamaterials from the linear response. *Nat. Mater*. **2015**, *14*, 379.

(14) Lee, J.; Tymchenko, M.; Argyropoulos, C.; Chen, P. Y.; Lu, F.; Demmerle, F.; Boehm, G.; Amann, M. C.; Alù, A.; Belkin, M. A. Giant nonlinear response from plasmonic metasurfaces coupled to intersubband transitions. *Nature* **2014**, *511*, 65-69.

(15) Hanke, T.; Krauss, G.; Trautlein, D.; Wild, B.; Bratschitsch, R.; Leitenstorfer, A. Efficient nonlinear light emission of single gold optical antennas driven by few-cycle near-infrared pulses. *Phys. Rev. Lett.* **2009**, *103*, 257404.

(16) Utikal, T.; Zentgraf, T.; Paul, T.; Rockstuhl, C.; Lederer, F.; Lippitz, M.; Giessen, H. Towards the origin of the nonlinear response in hybrid plasmonic systems. *Phys. Rev. Lett.* **2011**, *106*, 133901.

(17) Chen, S. M.; Li, G. X.; Zeuner, F.; Wong, W. H.; Pun, E. Y. B.; Zentgraf, T.; Cheah, K. W.; Zhang, S. Symmetry-Selective Third-Harmonic Generation from Plasmonic Metacrystals. *Phys. Rev. Lett.* **2014**, *113*, 033901.

(18) Aouani, H.; Rahmani, M.; Navarro-Cía, M.; Maier, S. A. Third-harmonic-upconversion enhancement from a single semiconductor nanoparticle coupled to a plasmonic antenna. *Nat. Nanotech.* **2014**, *9*, 290-294.

(19) Sederberg, S.; Elezzabi, A. Y. Coherent visible-light-generation enhancement in silicon-based nanoplasmonic waveguides via third-harmonic conversion. *Phys. Rev. Lett.* **2015**, *114*, 227401.

(20) Li, G. X.; Chen, S. M.; Pholchai, N.; Wong, W. H.; Pun, E.Y. B.; Cheah, K. W.; Zentgraf, T.; Zhang, S. Continuous control of the nonlinearity phase for harmonic generations. *Nat. Mater.* **2015**, *14*, 607-612.

(21) Renger, J.; Quidant, R.; Van Hulst, N.; Novotny, L. Surface-enhanced nonlinear four-wave mixing. *Phys. Rev. Lett.* **2010**, *104*, 046803.

(22) Rose, A.; Powell, D. A.; Shadrivov, I. V.; Smith, D. R.; Kivshar, Y. S. Circular dichroism of four-wave mixing in nonlinear metamaterials. *Phys. Rev. B* **2013**, *88*, 195148.

(23) Suchowski, H.; O'Brien, K.; Wong, Z. J.; Salandrino, A.; Yin, X.; Zhang, X. Phase mismatch free nonlinear propagation in optical Zero-Index materials. *Science* **2013**, *342*, 1223-1226.

(24) Corcoran, B.; Monat, C.; Grillet, C.; Moss, D. J.; Eggleton, B. J.; White, T. P.; O'Faolain, L.; Krauss T. F. Green light emission in silicon through slow-light enhanced third-harmonic generation in photonic-crystal waveguides. *Nat. Photon.* **2009**, *3*, 206-210.

(25) Galli, M.; Gerace, D.; Welna, K.; Krauss, T. F.; O'Faolain, L.; Guizzetti, G.; Andreani, L. C. Low-power continuous-wave harmonic generation in silicon photonic crystal cavities. *Opt. Express* **2010**, *18*, 26613-26624.

(26) Shcherbakov, M. R.; Neshev, D. N.; Hopkins, B.; Shorokhov, A. S.; Staude, I.; Melik-Gaykazyan, E. V.; Decker, M.; Ezhov, A. A.; Miroshnichenko, A. E.; Brener, I.; Fedyanin, A. A.; Kivshar, Y. S. Enhanced Third-Harmonic Generation in Silicon Nanoparticles Driven by Magnetic Response. *Nano Lett.* **2014**, *14*, 6488-6492.

(27) Yang, Y.; Wang, W.; Boulesbaa, A.; Kravchenko, I. I.; Briggs, D. P.; Puretzky, A.; Geohegan, D.; Valentine, J. Nonlinear Fano-Resonant Dielectric Metasurfaces. *Nano Lett.* **2015**, *15*, 7388-7393.

(28) Shcherbakov, M. R.; Shorokhov, A. S.; Neshev, D. N.; Hopkins, B.; Staude, I.; Melik-Gaykazyan, E. V.; Ezhov, A. A.; Miroshnichenko, A. E.; Brener, I.; Fedyanin, A. A.; Kivshar, Y. S. Nonlinear Interference and Tailorable Third-Harmonic Generation from Dielectric Oligomers. *ACS Photon.* **2015**, *2*, 578-582.

(29) Shorokhov, A. S.; Melik-Gaykazyan, E. V.; Smirnova, D. A.; Hopkins, B.; Chong, K. E.; Choi, D. Y.; Shcherbakov, M. R.; Miroshnichenko, A. E.; Neshev, D. N.; Fedyanin, A. A.; Kivshar, Y. S. Multifold Enhancement of Third-Harmonic Generation in Dielectric Nanoparticles Driven by Magnetic Fano Resonances. *Nano Lett.* **2016**, *16*, 4857-4861.

(30) Melik-Gaykazyan, E. V.; Shcherbakov, M. R.; Shorokhov, A. S.; Staude, I.; Brener, I.; Neshev, D. N.; Kivshar, Y. S.; Fedyanin, A. A. Third-harmonic generation from Mie-type resonances of isolated all-dielectric nanoparticles. *Phil. Trans. R. Soc. A* **2017**, *375*, 20160281.

(31) Wang, L.; Kruk, S.; Xu, L.; Rahmani, M.; Smirnova, D.; Solntsev, A.; Kravchenko, I.; Neshev, D. N.; Kivshar, Y. S. Shaping the third-harmonic radiation from silicon nanodimers. *Nanoscale* **2017**, *9*, 2201-2206.

(32) Grinblat, G.; Li, Y.; Nielsen, M. P.; Oulton, R. F.; Maier, S. A. Enhanced Third Harmonic Generation in Single Germanium Nanodisks Excited at the Anapole Mode. *Nano Lett.* **2016**, *16*, 4635–4640.

(33) Grinblat, G.; Li, Y.; Nielsen, M. P.; Oulton, R. F.; Maier, S. A. Efficient Third Harmonic Generation and Nonlinear Subwavelength Imaging at a Higher-Order Anapole Mode in a Single Germanium Nanodisk. *ACS Nano* **2017**, *11*, 953–960.

(34) Shibanuma, T.; Grinblat, G.; Albella, P.; Maier, S. A. Efficient Third Harmonic Generation from Metal–Dielectric Hybrid Nanoantennas. *Nano Lett.* **2017**, *17*, 2647–2651.

(35) Jain, A.; Moitra, P.; Koschny, T.; Valentine, J.; Soukoulis, C. M. Electric and Magnetic Response in Dielectric Dark States for Low Loss Subwavelength Optical Meta Atoms. *Adv. Opt. Mater.* **2015**, *3*, 1431-1438.

(36) Yang, Y.; Miroshnichenko, A. E.; Kostinski, S. V.; Odit, M.; Kapitanova, P.; Qiu, M.; Kivshar, Y. S. Multimode directionality in all-dielectric metasurfaces. *Phys. Rev. B* 2017, **95**, 165426.

Acknowledgments

This work was partly supported by EPSRC (EP/J018473/1), Leverhulme (Grant RPG-2012-674) EU-NOCTURNO collaboration and the Australian Research Council. This work was performed in part at the ACT node of the Australian National Fabrication Facility, a company established under the National Collaborative Research Infrastructure Strategy to provide nano and micro-fabrication facilities for Australia's researchers. S. M. was supported by Marie Curie Individual Fellowship (Grant H2020-MSCA-IF-703803-NonlinearMeta). G. L. would like to thank the financial support from Natural Science Foundation of Shenzhen Innovation Committee (Grant JCYJ20170412153113701) and the National Natural Science Foundation of China (Grant 11774145). We acknowledge useful discussions with Y. Kivshar.

Notes: S. M. and M. R. contribute equally.

Figures

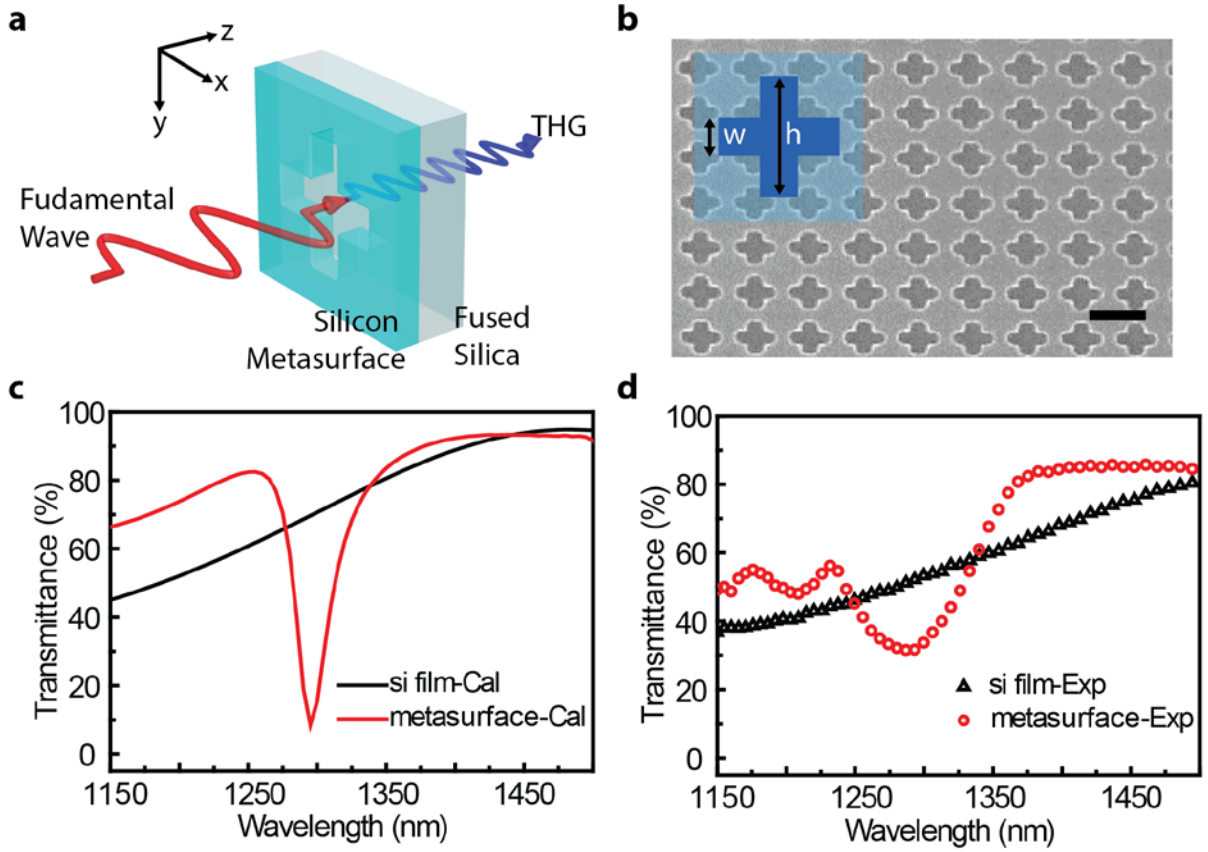

Figure 1. Geometry and transmission properties of the silicon metasurface. (a) Schematic view of a single silicon nanoaperture and (b) scanning electron microscopy image of the silicon metasurface (scale bar: 600 nm). The nanoaperture is milled into 205 nm thick silicon thin film using electron beam lithography and dry etching methods. The geometry parameters of the nanoaperture are w = 120 nm, h = 300 nm. (c) Calculated ('Cal') and (d) measured ('Exp') linear transmission spectra of the planar silicon film and metasurface for linearly (H-) polarized light, respectively. The calculated waveguide mode at wavelength around 1296 nm is also experimentally observed at wavelength around 1281 nm.

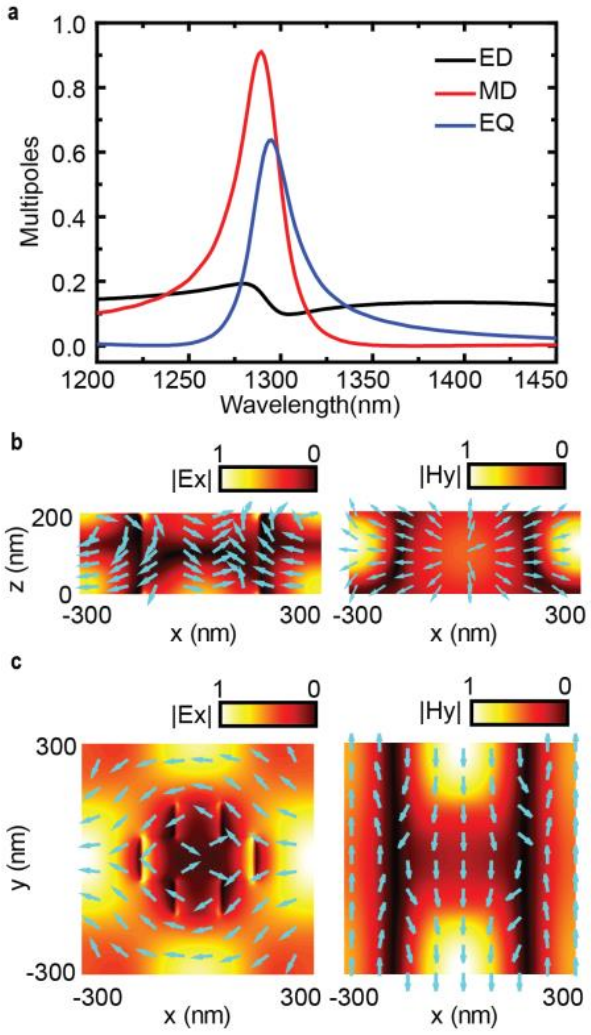

Figure 2. Linear optical response of the silicon metasurface. (a) Cartesian Multipolar analysis of optical modes ED: electric dipole; MD: Magnetic dipole; EQ: electric quadrupole. (b) and (c) Calculated field distribution of fundamental wave in a unit cell of the silicon metasurface. For linear (H-) polarized fundamental wave at wavelength of 1287 nm, the absolute values of electric field |Ex| and magnetic field |Hy| are plotted in X-Z (y=0) and X-Y (z=0) planes of a unit cell. In all the colour maps in (b) and (c), arbitrary unit was used.

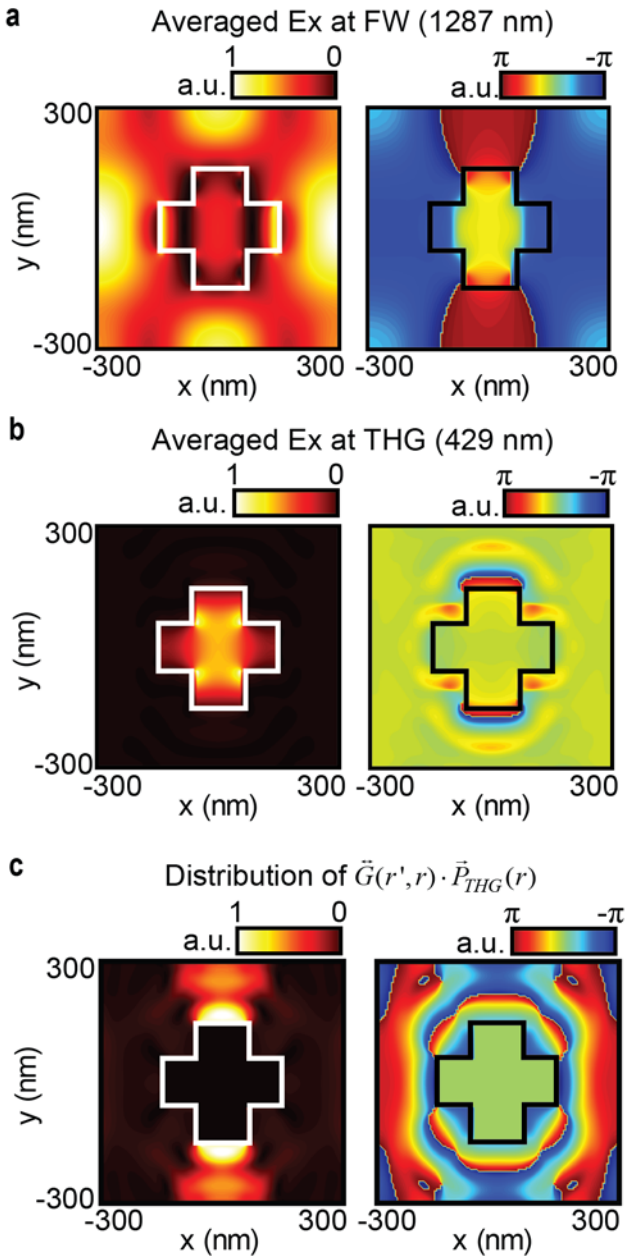

Figure 3. Contribution of the nonlinear polarization to the far field. The amplitude and phase distribution of (a) FW, (b) THG wave and (c) the local contribution to the far-field of THG intensity: $\ddot{G}(r',r)\cdot\vec{P}_{THG}(r)$ are plotted in X-Y plane. The fundamental and THG wavelengths are 1287 nm, 429 nm, respectively. Both the incident fundamental wave and the THG wave are TM-polarized.

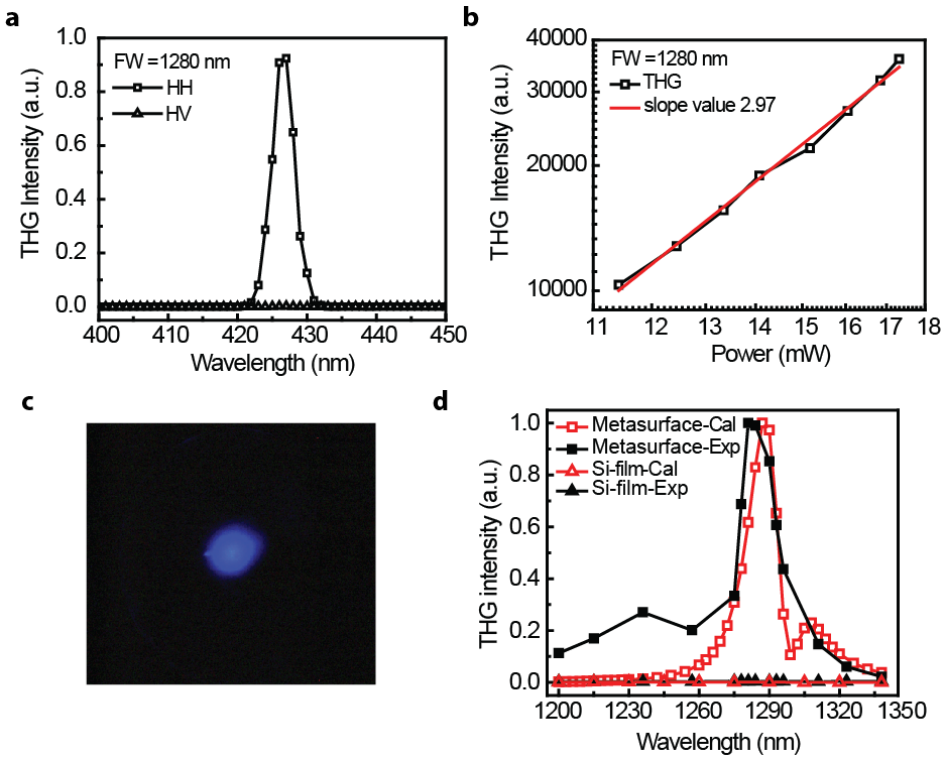

Figure 4. Characterization of third harmonic generation from silicon metasurface. (a) For linearly polarized (TM:H) fundamental waves at wavelength of 1280 nm which is normally incident onto the silicon metasurface, the spectra of THG with both same (H-H) and perpendicular polarization state (H-V) compared to that of the FW are measured. The THG signal for H-H measurement is much stronger (~ eight times) than that for the H-V configuration; (b) Power dependence of the THG intensity (open squares) for the H-H measurement. The result shows a cubic dependence (solid line) with slope value: ~ 3, which verifies the third order nonlinear optical process; (c) Typical THG radiation captured by colour CCD camera; (d) Measured ('Exp') THG spectra agree well with and calculated ('Cal') ones for both silicon planar film and metasurface. The measured giant THG enhancement occurs at wavelength of 1280 nm, which agrees with calculated peak THG value for FW at wavelength of 1287 nm.

For Table of Contents Use Only

Third harmonic generation enhanced by multipolar interference in complementary silicon metasurfaces

Shumei Chen[1♦], Mohsen Rahmani[2♦], King Fai Li[3], Andrey Miroshnichenko[4], Thomas Zentgraf[5], Guixin Li[3,6*], Dragomir Neshev[2*], Shuang Zhang[1*]